

## Volumetric quantification of bone-implant contact using micro-computed tomography analysis based on region-based segmentation

Sung-Won Kang<sup>1,†</sup>, Woo-Jin Lee<sup>1,†</sup>, Soon-Chul Choi<sup>2</sup>, Sam-Sun Lee<sup>2</sup>, Min-Suk Heo<sup>2</sup>, Kyung-Hoe Huh<sup>2</sup>, Tae-Il Kim<sup>3,\*</sup>, Won-Jin Yi<sup>2,\*</sup>

<sup>1</sup>Interdisciplinary Program in Radiation, Applied Life Science Major, College of Medicine, BK21, and Dental Research Institute, Seoul National University, Seoul, Korea

<sup>2</sup>Department of Oral and Maxillofacial Radiology, BK21, and Dental Research Institute, School of Dentistry, Seoul National University, Seoul, Korea

<sup>3</sup>Department of Periodontology and Dental Research Institute, School of Dentistry, Seoul National University, Seoul, Korea

### ABSTRACT

**Purpose:** We have developed a new method of segmenting the areas of absorbable implants and bone using region-based segmentation of micro-computed tomography (micro-CT) images, which allowed us to quantify volumetric bone-implant contact (VBIC) and volumetric absorption (VA).

**Materials and Methods:** The simple threshold technique generally used in micro-CT analysis cannot be used to segment the areas of absorbable implants and bone. Instead, a region-based segmentation method, a region-labeling method, and subsequent morphological operations were successively applied to micro-CT images. The three-dimensional VBIC and VA of the absorbable implant were then calculated over the entire volume of the implant. Two-dimensional (2D) bone-implant contact (BIC) and bone area (BA) were also measured based on the conventional histomorphometric method.

**Results:** VA and VBIC increased significantly with as the healing period increased ( $p < 0.05$ ). VBIC values were significantly correlated with VA values ( $p < 0.05$ ) and with 2D BIC values ( $p < 0.05$ ).

**Conclusion:** It is possible to quantify VBIC and VA for absorbable implants using micro-CT analysis using a region-based segmentation method. (*Imaging Sci Dent* 2015; 45: 7-13)

**KEY WORDS:** Absorbable Implants; Osseointegration; X-Ray Microtomography; Computer-Assisted Image Processing

### Introduction

In dental implant treatment, the surface characteristics and biocompatibility of implant materials are the most important factors in successful osseointegration.<sup>1</sup> Titanium is the most commonly used material for existing dental

implants because of its outstanding capacity for osseointegration. The installation of implants made with non-absorbable material in children still in their growth period can lead to lower sedimentation of the implant, caused by the growth of surrounding alveolar bone.<sup>2</sup> Moreover, a case report has been published describing how an ankylosed implant inhibited the alveolar bone, preventing it from undergoing the growth that was occurring elsewhere in the jaws.<sup>3</sup> Currently, no proper implant treatment method is available in pediatric dentistry for replacing lost deciduous teeth.

Absorbable implants can minimize the side effect of lower sedimentation, since the implant is absorbed internally after placement. We have been developing an implant made with absorbable material that can be absorbed even

\*This study was supported by a grant of the Korean Health Technology R&D Project, Ministry of Health & Welfare, Republic of Korea (HI13C1491).

Received July 10, 2014; Revised November 10, 2014; Accepted November 17, 2014

<sup>†</sup> Contributed equally to this study as the co-first author.

\*Correspondence to : Prof. Won-Jin Yi

Department of Oral and Maxillofacial Radiology, School of Dentistry, Seoul National University, Seoul, Korea

Tel) 8-22-2072-3049, Fax) 8-22-744-3919, E-mail) wjyi@snu.ac.kr

\*Correspondence to : Prof. Tae-Il Kim

Department of Periodontology, School of Dentistry, Seoul National University, Seoul, Korea

Tel) 82-2-2072-2642, Fax) 82-2-744-0051, E-mail) periopf@snu.ac.kr

in cases of lower sedimentation. Implants of bio-absorbable ceramics have already been used in orthopedics. Tricalcium phosphate (TCP) becomes part of the bone after being absorbed,<sup>4</sup> and polylactic acid (PLA) induces over 50% regeneration in regions with bone loss.<sup>5,6</sup> The strength reduction characteristic of a TCP implant can be minimized by conjunction with PLA.<sup>7</sup> Other synthetic biodegradable materials such as polyglycolic acid and polycaprolactone are able to undergo chemical decomposition in the body.

Osseointegration is critical to the success of dental implant treatment and has been well studied, with ongoing research and development.<sup>8,9</sup> The osseointegration capacity of implants made from non-absorbable material has been studied extensively.<sup>10-13</sup> Two-dimensional (2D) histomorphometric analysis has been widely used to examine thin specimens due to its high spatial resolution and contrast.<sup>14,15</sup> Bone-implant contact (BIC) and bone area (BA) have been quantitatively measured to evaluate osseointegration based on 2D histomorphometric images. However, the use of this technique to evaluate osseointegration has the disadvantages of requiring complex equipment and specimen preparation. Moreover, the rather destructive process of specimen fabrication makes it difficult to reproduce the specimen. Unfavorable changes or damage may also occur at the interface of the bone and the implant surface when preparing and sectioning the specimens. The most important disadvantage is that only a limited area can be analyzed, because most of the specimen is lost during preparation.

A three-dimensional (3D) analysis method using micro-computed tomography (micro-CT) images has been developed<sup>16-19</sup> and exhibits a high correlation with the results of histomorphometric analyses.<sup>20-22</sup> Generally, a threshold method is used in micro-CT analysis to separate the areas of the bone and the implant.<sup>16-22</sup> However, the simple threshold technique used in previous micro-CT analyses cannot be used to segment the areas of absorbable implant and bone, because the voxel intensities of the implants are similar to those of bone and the voxel intensity of the implants exhibits intrinsic inhomogeneity. Therefore, a new analytical technique is necessary to measure the osseointegration of absorbable implants.

In this study, we have developed a new method to segment the areas of absorbable implants and bone using region-based segmentation of micro-CT images. We evaluated the osseointegration of absorbable implants over the entire implant surface by analyzing segmented micro-CT images. The results of the micro-CT analysis for the

absorbable implants were compared with those obtained through histomorphometric analysis.

## Materials and Methods

In this study, we used a special implant developed for stable positioning and favorable bone regeneration. The upper part of the implant was manufactured with grade IV titanium, whereas the lower part was composed of a PLA-TCP nanocomposite (Fig. 1). The upper part of the implant had a mini-implant shape with a length of 5 mm and a diameter of 3.5 mm. Hybrid nanopowders, made of a 30% mixture of PLA-TCP, were melted into the nanocomposites to form the implant substructures. Seven beagle dogs (average age, 2 years; average weight, 13 kg) were used as experimental animals. All animal experiments, including animal management and surgical procedures, were approved and performed under the guidelines of the Institutional Animal Care and Use Committee of Seoul National University. Xylazine hydrochloride (Rumpen, Bayer Korea, Seoul, Korea) mixed with ketamine (Ketalar, Yuhan, Seoul, Korea) was injected into the veins of the dogs, and the second and fourth premolars were extracted from the left and right lower jaws. The operation was followed by an eight-week healing period. Three months after the extraction, 28 implants were placed. Seven implants broken during placement were excluded from the subsequent experiment. The animals were sacrificed four, eight, or 12 weeks after implant placement. The bones, including the implants, were cut to obtain samples, which were fixed in 10% formalin solution for

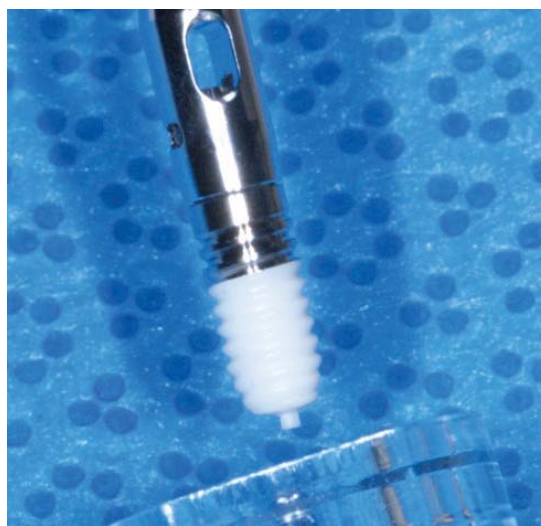


**Fig. 1.** An absorbable implant consists of a titanium upper part and a polylactic acid/tricalcium phosphate (PLA-TCP) lower part.

48 hours. The samples were scanned at 70 kVp and 141  $\mu$ A, using a Skyscan 1172 micro-CT scanner (Skyscan, Kontich, Belgium). The micro-CT image had a pixel size of 9.86  $\mu$ m and 12-bit depth. A non-placed implant was also scanned for use as a control image.

The micro-CT images were processed to separate the implant area from the bone area for the quantitative 3D analysis of osseointegration. The areas of the bone and implant were segmented by a region-based method, using a region-growing algorithm.<sup>23</sup> This method segmented the bone and implant by taking a seed region as the initial segmentation, and then iteratively added all the connected voxels whose intensity fell within a dynamically defined range.<sup>23</sup> Holes were generated inside the implant area, as the seed boundary values of the segmentation did not include TCP particles with greater than normal brightness. The holes were filled using a region-labeling method<sup>24</sup> that automatically merged similar segmented regions.

The overall procedure for separating the implant area from the bone area was as follows. First, the reconstructed image was passed through a smoothing process, using a curvature flow filter to reduce the influence of noise (Figs. 2A and F). The images were then segmented into bone and implant areas using an area-based confidence connected segmentation method (Figs. 2B and G).<sup>23</sup> After segmenting the implant area, holes were generated inside the implant area (Figs. 2C and H). The holes were filled using a region-labeling method (Figs. 2D and I).<sup>24</sup> The boundary between the bone and implant areas was smooth-

ed using the morphological operations of erosion and dilation. If one of the four-connected neighbors of a pixel in the implant area was a bone pixel, that pixel was determined to belong to the area of bone-implant contact (Figs. 2E and J). The segmented areas of the bone and implant underwent 3D reconstruction after all steps of the image processing were applied to the axial slices of the micro-CT images.

The volumetric absorption (VA) of an implant was calculated by comparing it to the volume of a reference implant that was not placed (Eq. 1). The volumetric bone-implant contact (VBIC) ratio was defined by comparing the area of the implant surface boundary in direct contact with the bone to the total area of the implant surface (Eq. 2). The VBIC ratio was calculated over the entire surface area of the implant, not over a partial sample of selected threads. All parameters were measured only for the volume of the lower absorbable implant, after the titanium in the upper portion of the implant was excluded.

$$VA = \left(1 - \frac{V_{imp}}{V_{ref}}\right) \times 100 \quad (1)$$

$V_{ref}$ : the total volume of the reference implant not placed  
 $V_{imp}$ : the total volume of the placed implant

$$VBIC = \left(\frac{S_{bone}}{S_{imp}}\right) \times 100 \quad (2)$$

$S_{bone}$ : the area of the implant surface in contact with bone  
 $S_{imp}$ : the total of the implant surface

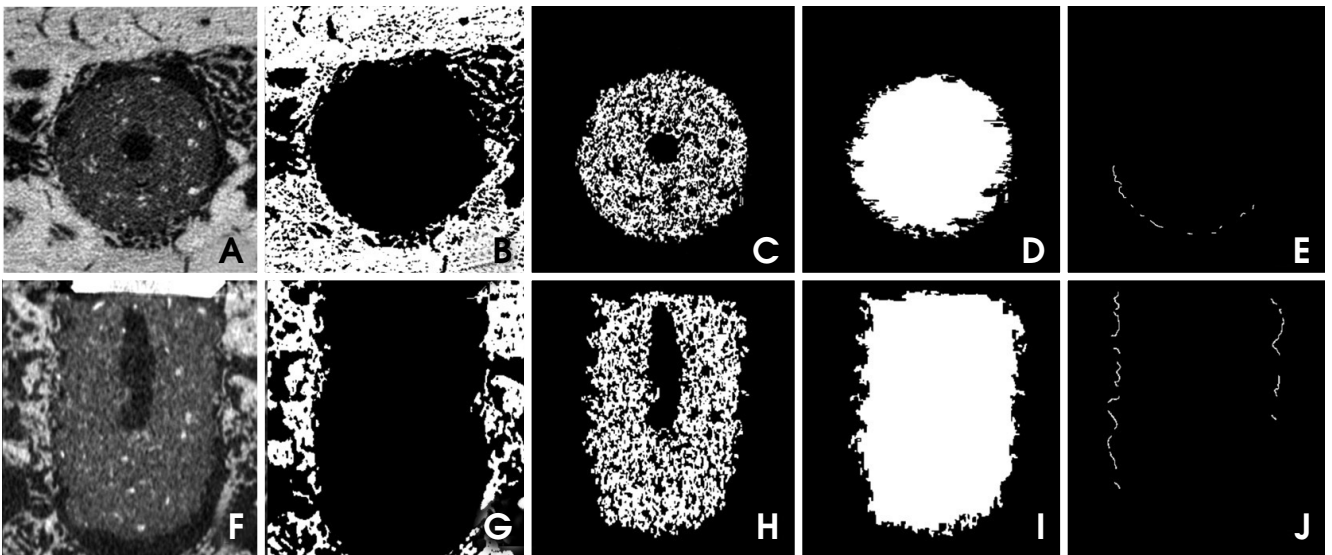


**Fig. 2.** Smoothed micro-computed tomography image of the absorbable implant in axial (A) and coronal (F) slices. Segmented images of the bone in axial (B) and coronal (G) slices. Segmented images of the implant in axial (C) and coronal (H) slices. Hole-filled images of the implant in axial (D) and coronal (I) slices. The implant surface in direct contact with the bone in axial (E) and coronal (J) slices

The samples were also sliced for 2D histomorphometric analysis. 2D optical images of the slices were analyzed and recorded at a magnification of 100× using an optical microscope (BH-2TM, Olympus Optical, Osaka, Japan). The images were analyzed with the ScopeEye image analysis software (Tecsan, Seoul, Korea). 2D BIC and BA were measured based on the conventional histomorphometric method.<sup>25</sup> For statistical analysis, ANOVA was performed using SPSS version 19 (SPSS Inc., Chicago, IL, USA) in order to evaluate variation in the mean implant healing period. Pearson’s correlation analysis was also performed to assess correlations between the 3D and 2D measurements.

### Results

Table 1 shows the distribution of the implants that were used for analysis and placed in the lower jaw of the beagle dogs. The reconstructed volumes of bone and the implants after segmentation were rendered in 3D, and the 3D reconstructed images were organized to reflect variation in the healing period (Fig. 3). In the images, we observed an increase in implant absorption as the healing period increased. The extent of absorption of an implant after eight weeks was shown to be quite different from that indicated by the initial 3D implant thread positions. The mean VA values of the implant area were 23.46 ± 5.25% at four weeks, 38.89 ± 2.46% at eight weeks, and 41.94 ± 4.51% at

12 weeks after implant placement, showing a significant increase as the healing period was extended ( $p < 0.05$ ) (Table 2). The mean VBIC values were 17.67 ± 3.20% at four weeks, 25.23 ± 4.36% at eight weeks, and 36.18 ± 4.33% at 12 weeks. The mean VBIC also increased significantly as the healing period increased ( $p < 0.05$ ) (Table 2).

The mean 2D BA values according to histomorphometric analysis were 62.07 ± 8.43% at four weeks, 72.25 ± 27.91% at eight weeks, and 82.01 ± 21.34 % at 12 weeks after implant placement (Fig. 4). The BA values increased over time, but did not show a statistically significant

**Table 1.** Distribution of the placed implants used for analysis

Period	Implantation site	Number
4 weeks	Second premolar	4
	Fourth premolar	4
8 weeks	Second premolar	3
	Fourth premolar	4
12 weeks	Second premolar	3
	Fourth premolar	3

**Table 2.** Volumetric absorption (VA) and volumetric bone-implant contact (VBIC) of the absorbable implants evaluated with micro-CT analysis, by treatment period (mean ± SD)

Period	4 weeks	8 weeks	12 weeks
VA (%)	23.46 ± 5.25	38.89 ± 2.46	41.94 ± 4.51
VBIC (%)	17.67 ± 3.20	25.23 ± 4.36	36.18 ± 4.33

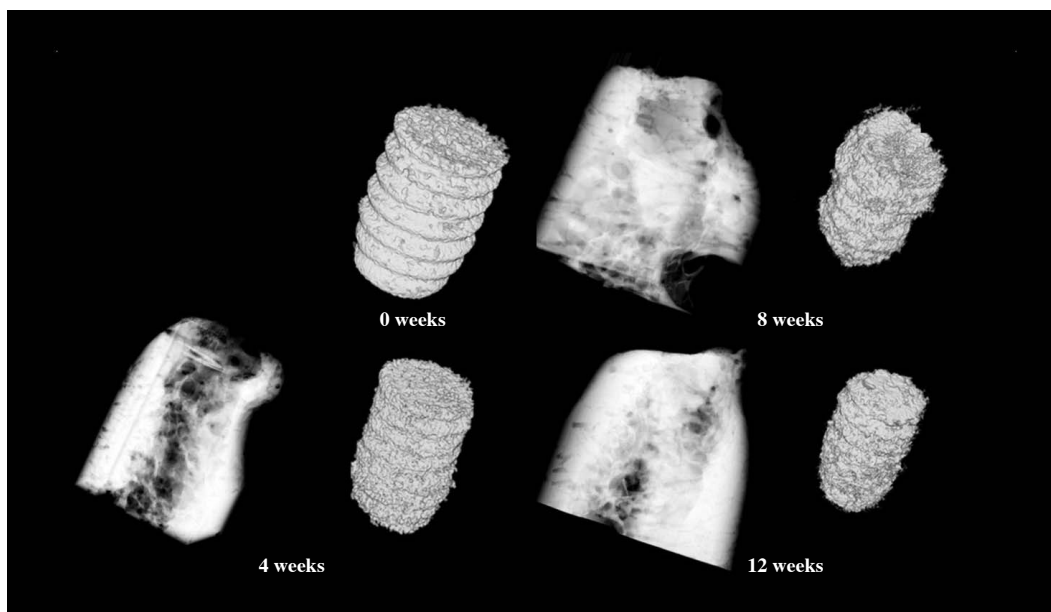


**Fig. 3.** Three-dimensional rendering of the reconstructed volumes shows the bone and implant after segmentation.

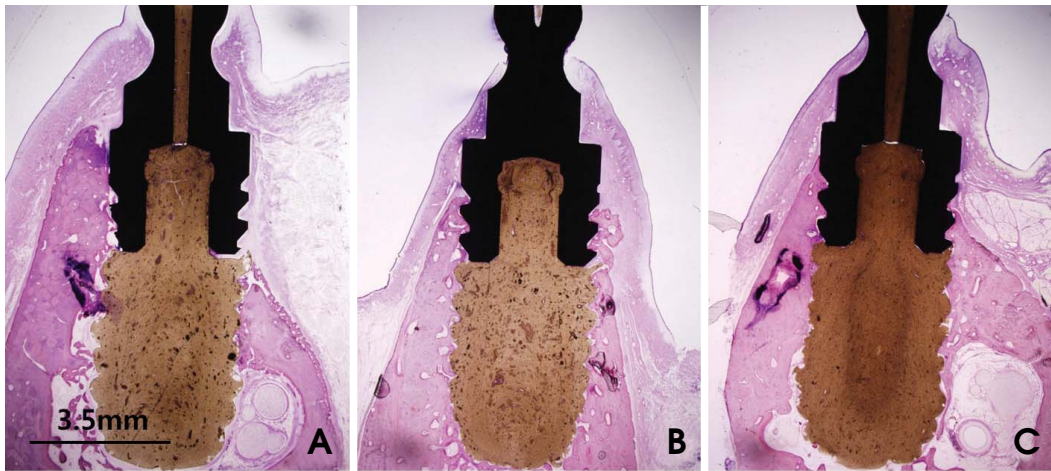


**Fig. 4.** Histomorphometric images show the absorbable implant (100 ×) at four weeks (A), eight weeks (B), and 12 weeks (C) after placement.

**Table 3.** Two-dimensional bone area (BA) and bone-implant contact (BIC) of the absorbable implants, evaluated with histomorphometric analysis, by treatment period (mean ± SD).

Period	4 weeks	8 weeks	12 weeks
BA (%)	62.07 ± 8.43	72.25 ± 27.91	82.01 ± 21.34
BIC (%)	30.57 ± 6.59	32.20 ± 9.13	35.50 ± 10.63

ificant relationship with the length of the healing period ( $p > 0.05$ ) (Table 3). The mean 2D BIC values were  $30.57 \pm 6.59\%$  at four weeks,  $32.20 \pm 9.13\%$  at eight weeks, and  $35.50 \pm 10.63\%$  at 12 weeks. Similarly to the BA values, the BIC values increased over time, but this relationship was not statistically significant ( $p > 0.05$ ) (Table 3). Table 4 shows the Pearson's correlation coefficients between the 3D micro-CT measurements and the results of 2D histomorphometric analysis. VBIC was highly significantly correlated with VA ( $p < 0.05$ ) (Fig. 5) and was significantly correlated with 2D BIC ( $p < 0.05$ ). 2D BA exhibited no correlations with the other parameters.

## Discussion

Surgical technique, quality and quantity of bone, and osseointegration of the implant are important factors in successful implant treatment. In particular, osseointegration is known to be affected by factors such as the surface characteristics and biological compatibility of an implant.<sup>1</sup> Increased roughness on the surface of an implant tends to increase BIC.<sup>26,27</sup> The recently developed method of acid etching uses surface corrosion to increase osseointegration.<sup>28,29</sup> There has been less interest in assessing implant

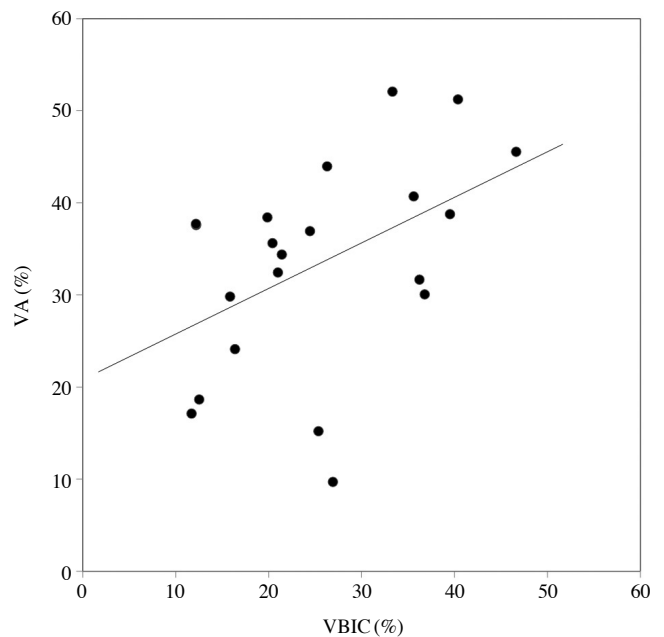


**Fig. 5.** The relationship between the volumetric bone-implant contact ratio (VBIC, %) and volumetric absorption (VA, %) (Pearson's correlation = 0.46,  $p < 0.05$ ).

treatment in the jaws of children than in the jaws of adults. It is necessary to develop implants that can be used for the treatment of congenital and accidental tooth loss during the growth phase. The installation of implants made with non-absorbable material in children can lead to lower sedimentation of the implant, caused by the growth of the surrounding alveolar bone.<sup>2</sup> In addition to this, ankylosed implants may inhibit the alveolar bone, preventing it from undergoing the growth experienced elsewhere in the jaws.<sup>3</sup>

**Table 4.** Pearson’s correlation coefficients between two-dimensional histomorphometric and three-dimensional micro-CT analyses, including bone-implant contact ratio (BIC), bone area (BA), volumetric bone-implant contact ratio (VBIC), and volumetric absorption (VA)

	BIC	BA	VBIC	VA
BIC		0.03 (0.45)	0.34 (0.05)*	0.31 (0.07)
BA	0.03 (0.45)		0.26 (0.87)	0.33 (0.68)
VBIC	0.34 (0.05)*	0.26 (0.87)		0.46 (0.00)*
VA	0.31 (0.07)	0.33 (0.68)	0.46 (0.00)*	

\*p&lt;0.05

Absorbable implants can minimize the side effect of lower sedimentation, since the implant is absorbed internally after placement. We have been developing an implant made of absorbable material that can be absorbed even in cases of lower sedimentation. This new type of implant is currently under a preclinical trial in order to gather more data that would justify a clinical trial.

In general, a threshold method is used in micro-CT analysis to segment the areas of the bone and implant.<sup>16-22</sup> An adequate threshold for the bone and implant is selected by superimposing segmented images over the original grayscale images.<sup>30,31</sup> The threshold technique used in micro-CT analysis cannot be used to separate areas of absorbable implant and bone. The histogram of these areas does not present the clear bimodal characteristics of metal implants, because the voxel intensities of absorbable implant material are similar to those of bone in micro-CT images. Additionally, the absorbable implant area displays an intrinsic inhomogeneity of voxel intensities that is not found in areas with a metal implant, since absorbable implants are composed of composite materials. Therefore, if an absorbable implant is present, is not possible to accomplish segmentation by directly using the threshold method, which is based on the presence of homogeneous voxel intensities. In order to solve these issues, we employed a region-based segmentation method that uses region-growing and region-labeling algorithms. Finally, the area of bone-implant contact determined by the segmentation results was validated by visual inspection after superimposing the contact area over the original unsegmented image. We were able to determine the area of bone-implant contact over the entire surface of the implant by segmenting the micro-CT images with inhomogeneous voxel intensities using the region-based method.

Evaluations of BA and BIC through histomorphometric analysis are the parameters most widely used to measure osseointegration. In this study, histomorphometric analy-

sis did not show that the BA and BIC of the absorbable implant significantly increased during the healing process. The exact positioning of the absorbable implant thread and its radius setting were difficult to measure in the 2D histomorphometric analysis of BA and BIC, because the thread morphology of the implant changed during healing through processes of absorption and distortion. This difficulty may have resulted in the lack of statistical significance. In order to overcome these problems in the histomorphometric analysis, the entire volume of the implant was taken into account when calculating the VBIC ratio and VA using micro-CT analysis. The 3D VBIC ratio and VA, as measured by the micro-CT method, increased significantly during healing. Moreover, the 3D measurements of VBIC and VA using the micro-CT analysis were highly correlated with each other, despite continuous changes in the morphology of the implant. This implies that the 3D osseointegration and absorption of the absorbable implant increase simultaneously at the implant surface during healing.

Nonetheless, the 3D VBIC ratio for the absorbable implant was significantly correlated with 2D BIC. However, other correlations among the results of the two methods were weak. The histomorphometric analysis provided only 2D measurements for the sectioned slices. Measurements using only fractional slices cannot indicate the total absorption or total BIC of the absorbable implant. The lack of statistical significance regarding osseointegration over time and the lack of correlation between the two measurement systems may have been caused by the inherent limitations of histomorphometric analysis, which is based on 2D measurements.

In conclusion, we were able to quantify VBIC and VA for an absorbable implant using micro-CT analysis based on a region-based segmentation method. Osseointegration was evaluated over the entire surface of the implant, which may overcome some limitations of histomorphometric analysis applied to absorbable implants. In future studies, we will apply the method described here to overcome the limitations of micro-CT analysis of the BIC around metal implants. These limitations are mainly related to metal artifacts in computed tomography images, and overcoming them may enable the more accurate assessment of VBIC in metal implants.

## References

1. Schnitman PA, Wöhrle PS, Rubenstein JE, DaSilva JD, Wang NH. Ten-year results for Brånemark implants immediately

- loaded with fixed prostheses at implant placement. *Int J Oral Maxillofac Implants* 1997; 12: 495-503.
2. Rossi E, Andreassen JO. Maxillary bone growth and implant positioning in a young patient: a case report. *Int J Periodontics Restorative Dent* 2003; 23: 113-9.
  3. Tarlow JL. The effect of adult growth on an anterior maxillary single-tooth implant: a clinical report. *J Prosthet Dent* 2004; 92: 213-5.
  4. Laffargue P, Fialdes P, Frayssinet P, Rtaimate M, Hildebrand HF, Marchandise X. Adsorption and release of insulin-like growth factor-I on porous tricalcium phosphate implant. *J Biomed Mater Res* 2000; 49: 415-21.
  5. Robert P, Mauduit J, Frank RM, Vert M. Biocompatibility and resorbability of a polylactic acid membrane for periodontal guided tissue regeneration. *Biomaterials* 1993; 14: 353-8.
  6. Kulkarni RK, Pani KC, Neuman C, Leonard F. Polylactic acid for surgical implants. *Arch Surg* 1966; 93: 839-43.
  7. Karabuda C, Ozdemir O, Tosun T, Anil A, Olgaç V. Histological and clinical evaluation of 3 different grafting materials for sinus lifting procedure based on 8 cases. *J Periodontol* 2001; 72: 1436-42.
  8. Brånemark PI, Hansson BO, Adell R, Breine U, Lindström J, Hallén O, et al. Osseointegrated implants in the treatment of the edentulous jaw. Experience from a 10-year period. *Scand J Plast Reconstr Surg Suppl* 1977; 16: 1-132.
  9. Albrektsson T, Brånemark PI, Hansson HA, Lindström J. Osseointegrated titanium implants. Requirements for ensuring a long-lasting, direct bone-to-implant anchorage in man. *Acta Orthop Scand* 1981; 52: 155-70.
  10. Kim DS, Kim DG, Park CJ, Cho LR. Histomorphometry and stability analysis of early loaded implants with two different surface conditions in beagle dogs. *J Adv Prosthodont* 2009; 1: 10-8.
  11. Nkenke E, Hahn M, Weinzierl K, Radespiel-Troger M, Neukam FW, Engelke K. Implant stability and histomorphometry: a correlation study in human cadavers using stepped cylinder implants. *Clin Oral Implants Res* 2003; 14: 601-9.
  12. Deguchi T, Nasu M, Murakami K, Yabuuchi T, Kamioka H, Takano-Yamamoto T. Quantitative evaluation of cortical bone thickness with computed tomographic scanning for orthodontic implants. *Am J Orthod Dentofacial Orthop* 2006; 129: 721.e7-12.
  13. Garetto LP, Chen J, Parr JA, Roberts WE. Remodeling dynamics of bone supporting rigidly fixed titanium implants: a histomorphometric comparison in four species including humans. *Implant Dent* 1995; 4: 235-43.
  14. Roberts WE. Bone tissue interface. *J Dent Educ* 1988; 52: 804-9.
  15. Le Guehennec L, Goyenvale E, Lopez-Heredia MA, Weiss P, Amouriq Y, Layrolle P. Histomorphometric analysis of the osseointegration of four different implant surfaces in the femoral epiphyses of rabbits. *Clin Oral Implants Res* 2008; 19: 1103-10.
  16. Rebaudi A, Koller B, Laib A, Trisi P. Microcomputed tomographic analysis of the peri-implant bone. *Int J Periodontics Restorative Dent* 2004; 24: 316-25.
  17. Park HS, Kwon OW, Sung JH. Microscrew implant anchorage sliding mechanics. *World J Orthod* 2005; 6: 265-74.
  18. Schicho K, Kastner J, Klingsberger R, Seemann R, Enislidis G, Undt G, et al. Surface area analysis of dental implants using micro-computed tomography. *Clin Oral Implants Res* 2007; 18: 459-64.
  19. Van Oosterwyck H, Duyck J, Vander Sloten J, Van der Perre G, Jansen J, Wevers M, et al. Use of microfocus computerized tomography as a new technique for characterizing bone tissue around oral implants. *J Oral Implantol* 2000; 26: 5-12.
  20. Bernhardt R, Kuhlisch E, Schulz MC, Eckelt U, Stadlinger B. Comparison of bone-implant contact and bone-implant volume between 2D-histological sections and 3D-SRµCT slices. *Eur Cell Mater* 2012; 23: 237-48.
  21. Park YS, Yi KY, Lee IS, Jung YC. Correlation between microtomography and histomorphometry for assessment of implant osseointegration. *Clin Oral Implants Res* 2005; 16: 156-60.
  22. Liu S, Broucek J, Virdi AS, Sumner DR. Limitations of using micro-computed tomography to predict bone-implant contact and mechanical fixation. *J Microsc* 2012; 245: 34-42.
  23. Debats OA, Litjens GJ, Barentsz JO, Karssemeijer N, Huisman HJ. Automated 3-dimensional segmentation of pelvic lymph nodes in magnetic resonance images. *Med Phys* 2011; 38: 6178-87.
  24. Singh UP, Saxena K, Jain S. Semi-supervised method of multiple object segmentation with a region labeling and flood fill. *Signal Image Process* 2011; 2: 175-93.
  25. Park JW, An CH, Jeong SH, Suh JY. Osseointegration of commercial microstructured titanium implants incorporating magnesium: a histomorphometric study in rabbit cancellous bone. *Clin Oral Implants Res* 2012; 23: 294-300.
  26. Piattelli M, Scarano A, Paolantonio M, Iezzi G, Petrone G, Piattelli A. Bone response to machined and resorbable blast material titanium implants: an experimental study in rabbits. *J Oral Implantol* 2002; 28: 2-8.
  27. Buser D, Schenk RK, Steinemann S, Fiorellini JP, Fox CH, Stich H. Influence of surface characteristics on bone integration of titanium implants. A histomorphometric study in miniature pigs. *J Biomed Mater Res* 1991; 25: 889-902.
  28. Jeong R, Marin C, Granato R, Suzuki M, Gil JN, Granjeiro JM, et al. Early bone healing around implant surfaces treated with variations in the resorbable blasting media method. A study in rabbits. *Med Oral Patol Oral Cir Bucal* 2010; 15: e119-25.
  29. Rohner D, Tay A, Chung SM, Huttmacher DW. Interface of unloaded titanium implants in the iliac crest, fibula, and scapula: a histomorphometric and biomechanical study in the pig. *Int J Oral Maxillofac Implants* 2004; 19: 52-8.
  30. Butz F, Ogawa T, Chang TL, Nishimura I. Three-dimensional bone-implant integration profiling using micro-computed tomography. *Int J Oral Maxillofac Implants* 2006; 21: 687-95.
  31. Ko CY, Lim DH, Choi BH, Li J, Kim HS. Suggestion of new methodology for evaluation of osseointegration between implant and bone based on  $\mu$ -CT images. *Int J Precis Eng Man* 2010; 11: 785-90.